

CO₂ laser-grooved long period fiber grating temperature sensor system based on intensity modulation

Yi-Ping Wang, Dong Ning Wang, and Wei Jin

A long period fiber grating (LPFG) temperature sensor system based on intensity modulation is developed. The LPFG employed is fabricated by the use of a focused CO₂ laser beam to carve periodic grooves on the fiber. The temperature measurement resolution of up to 0.1 °C has been obtained within the temperature range between 20 °C and 100 °C. The system uses a simple intensity measurement method and exhibits the advantages of convenient intensity measurement, double temperature sensitivity, high resolution, simple configuration, and low cost. © 2006 Optical Society of America
OCIS codes: 060.2370, 060.2340, 050.2770.

1. Introduction

A long period fiber grating (LPFG) is a passive optical fiber device with a periodic refractive index modulation that couples the guided fundamental mode in the core to a forward-propagating cladding mode. This mode decays rapidly due to scattering at the cladding-air interface and the bend in the fiber. Because the resonant wavelength and coupling coefficient of LPFGs are dependent on temperature, strain, and refractive index of the surrounding material,^{1,2} LPFGs have been widely applied in optical fiber sensors. Such sensors exhibit advantages such as electromagnetic immunity, low backward reflection, and compactness. However, LPFG temperature sensors currently used are based on the measurement of the temperature-induced wavelength shift,²⁻⁴ which needs expensive equipment such as an optical spectrum analyzer, and is not suitable for practical applications in some cases. A more practical solution reported is through the use of intensity modulation.^{5,6} However, the LPFG was used only as an edge filter in the system, instead of a sensing element.

We present a novel LPFG temperature sensor system based on intensity modulation. The LPFG em-

ployed is fabricated by use of a focused CO₂ beam to carve periodic grooves on standard single mode fiber. The temperature resolution of up to 0.1 °C has been obtained within the temperature range between 20 °C and 100 °C. The system is simple, low cost, and easy to operate.

2. Long Period Fiber Grating Fabrication

Davis *et al.*,⁷ Rao *et al.*,⁸ and Wang and Rao⁹ reported LPFG fabrication techniques based on CO₂ laser-induced residual stress relaxation and the thermal shock effect from high-frequency CO₂ laser pulses. Here a novel LPFG is fabricated by the focused CO₂ laser beam carving periodic grooves on common optical fiber (Corning SMF-28). The fabrication setup employed is similar to that illustrated by Fig. 1 in Ref. 8. By use of a 2D optical scanner under computer control, the focused CO₂ laser beam scans repeatedly at the location, corresponding to the first grating period, of the fiber along the *X* direction. Then the laser beam is shifted by a grating pitch along the *Y* direction and scanned repeatedly to fabricate the next grating period. This scan and shift process is done periodically for *N* times (*N* is the number of grating periods) until the final grating period is fabricated. The repeat scanning of the focused CO₂ laser beam induces a local high temperature in the fiber, which leads to the gasifying of SiO₂ on the surface of the fiber. As a result, periodic grooves are created on the fiber as shown in Fig. 1. Such grooves induce periodic refractive index modulations along the fiber axis due to the photoelastic effect, thus creating a LPFG.

The groove's depth, which indicates the efficiency of CO₂ laser heating and the change of refractive index, is dependent on many fabrication parameters,

Y.-P. Wang (ypwang@china.com), D. N. Wang (eednwang@polyu.edu.hk), and W. Jin (eewjin@polyu.edu.hk) are with the Department of Electrical Engineering, Hong Kong Polytechnic University, Kowloon, Hong Kong, China. Y.-P. Wang is also with the State Key Laboratory of Advanced Optical Communication Systems and Networks, Shanghai Jiao Tong University, Shanghai 200240, China.

Received 1 May 2006; revised 14 June 2006; accepted 23 June 2006; posted 29 June 2006 (Doc. ID 70483).

0003-6935/06/317966-05\$15.00/0

© 2006 Optical Society of America

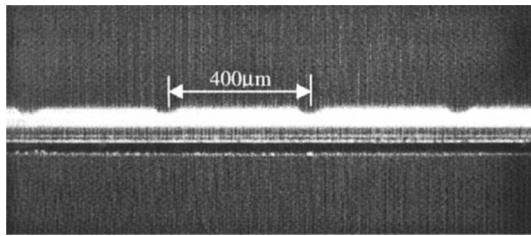


Fig. 1. Photograph of a CO₂ laser-grooved LPFG with a grating pitch of 400 μm observed by the CCD camera. Typical depth and width of the groove are approximately 15 and 50 μm, respectively.

such as the diameter of the focused laser light spot, the scanning speed, the average laser output power, the pulse frequency, and the number of scanning times at each groove location. During our fabrication process, the CO₂ laser beam was focused on a small spot with a diameter of only ~35 μm and scanned repeatedly at each grating groove location, which effectively enhances the heating efficiency of the CO₂ laser. As a result, periodic grooves are carved on the fiber by the CO₂ laser beam with a relatively low average output power of ~0.5 W. The laser beam scanning speed of 2.326 mm/s and the pulse frequency of 10 kHz were applied.

There was no physical deformation in the LPFGs fabricated by Davis *et al.*⁷ and Rao *et al.*,⁸ whereas periodic grooves are carved on our LPFGs, which is a unique feature of our fabrication technique. Such grooves have essentially no contribution to the LPFG's insertion loss, which is similar to the case of a corrugated LPFG produced by hydrofluoric acid etching.¹⁰ This is because these periodic grooves are totally confined within the fiber cladding and have no effect on the light transmission in the fiber core. As long as the grooves do not touch the central region near the fiber core, no obvious insertion loss is observed. Note that the typical depth and width of grooves are approximately 15 and 50 μm, respectively. The insertion losses of our LPFGs are due mainly to the nonperiodicity and the disorder of the refractive index change. As a result, LPFGs with a low insertion loss of less than 0.5 dB can be fabricated by the technique proposed.

Refractive index modulation in the CO₂ laser-grooved LPFG fabrication can be expressed as

$$\Delta n = \Delta n_{\text{residual}} + \Delta n_{\text{groove}}, \quad (1)$$

where $\Delta n_{\text{residual}}$ is the refractive index perturbation induced by residual stress relaxation resulting from the high local temperature, which is approximate to that of the CO₂ laser-induced LPFGs without periodic grooves^{7,8}; Δn_{groove} is the refractive index perturbation induced by the strain field resulting from grooves on the fiber, which is similar to that, i.e., $\Delta n_{\text{corrugated}}$, of the corrugated LPFGs fabricated by hydrofluoric acid etching.¹⁰ It can be seen from Eq. (1) that the refractive index modulation in the CO₂ laser-grooved LPFG is higher than that of the CO₂ laser-induced LPFG without periodic grooves. Therefore periodic grooves

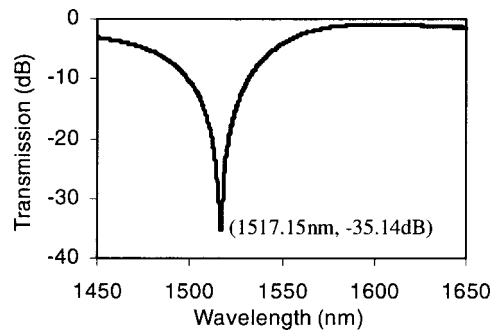


Fig. 2. Transmission spectrum of the CO₂ laser-grooved LPFG with a grating pitch of 400 μm and a number of grating periods of 20.

on the fiber effectively enhance the modulation efficiency of the refractive index. As a result a LPFG with a resonant wavelength of 1517.15 nm, a large transmission attenuation of up to -35.14 dB, and a low insertion loss of down to 0.3 dB was obtained, as shown in Fig. 2. In contrast the peak transmission attenuation of LPFGs without periodic grooves is typically approximately -25 dB.^{7,8}

3. Temperature Characteristics of Long Period Fiber Gratings

The CO₂ laser-grooved LPFG developed in this work combines the features of a CO₂ laser-induced LPFG without physical deformation and a corrugated LPFG fabricated by hydrofluoric acid etching. A column oven (LCO 102) with a temperature resolution of 0.1 °C and a photonic all-parameter analyzer (Agilent 81910A) were used to test the temperature characteristics of the LPFG. As shown in Figs. 3 and 4, with the temperature increasing the resonant wavelength of the LPFG shifts linearly toward the longer wavelength side with a sensitivity of 0.07 nm/°C and the peak transmission loss at the resonant wavelength increases. Thus the CO₂ laser-grooved LPFG can be used as a temperature sensor based on wavelength measurement, as reported in Refs. 2 and 3. It was observed previously by Rao *et al.*⁸ and Wang

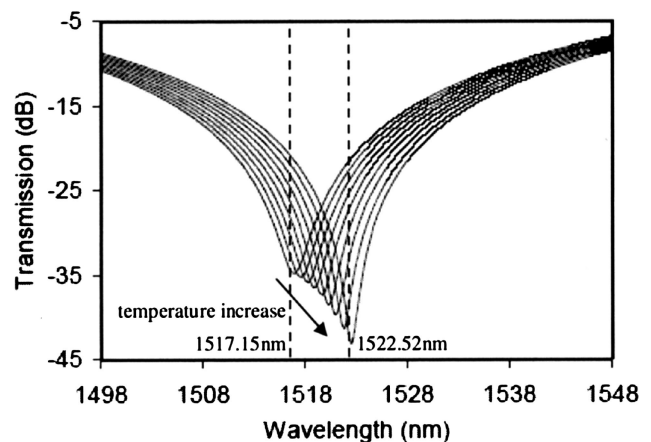


Fig. 3. Transmission spectra evolution of the LPFG when the temperature is increased from 20 °C to 100 °C in steps of 10 °C.

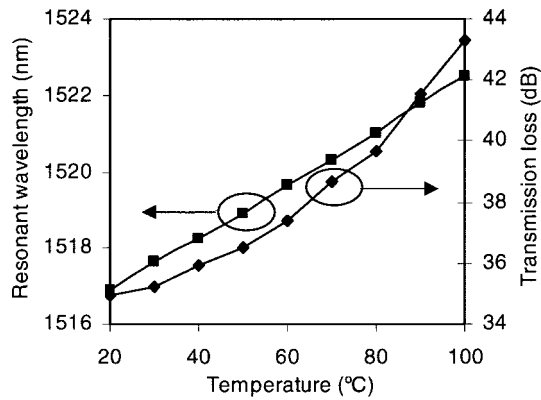


Fig. 4. Changes of the resonant wavelength and the transmission loss at the resonant wavelength of the LPFG when the temperature is increased from 20 °C to 100 °C in steps of 10 °C.

*et al.*¹¹ that, as the temperature increased, the peak transmission loss of the CO₂ laser-induced LPFG without periodic grooves hardly changed except that the wavelength shifted. In contrast, as shown in Figs. 3 and 4, the peak transmission loss of the CO₂ laser-grooved LPFG increases from 35.14 to 43.58 dB as the temperature increases. This unique temperature characteristic of the CO₂ laser-induced LPFG enhances the temperature sensitivity of the LPFG sensor based on intensity modulation.

It can be observed from Fig. 3 that, when the temperature is increased, the LPFG-induced loss decreases at the shorter wavelength than the resonant wavelength of 1517.15 nm and increases at the longer wavelength than the resonant wavelength of 1522.52 nm. For example, when the temperature is increased, the LPFG-induced loss decreases at wavelengths of 1500, 1504, 1508, 1512, and 1516 nm, and increases at wavelengths of 1523, 1527, 1531, 1535, and 1539 nm, as shown in Fig. 5. It can also be seen from Figs. 3 and 5 that, with the in-

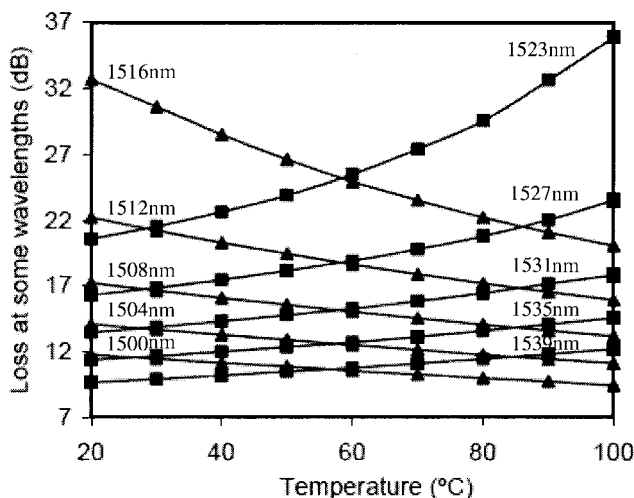


Fig. 5. Changes of the LPFG-induced loss at wavelengths of 1500, 1504, 1508, 1512, 1516, 1523, 1527, 1531, 1535, and 1539 nm when the temperature is increased from 20 °C to 100 °C in steps of 10 °C.

crease of the temperature, the LPFG-induced loss changes almost linearly at wavelengths shorter than 1508 nm and longer than 1531 nm.

4. Temperature Sensor System

From the linear relationship between the temperature and the transmission loss of the LPFG in a specified wavelength range, as shown in Fig. 6, a CO₂ laser-grooved LPFG temperature sensor system based on intensity modulation is developed. The broadband light source used is a LED that exhibits a symmetrical spectrum near the center wavelength λ_0 . The light from the LED is equally divided by a 3 dB coupler and illuminates two fiber Bragg gratings (FBGs) with Bragg wavelengths of λ_1 and λ_2 , respectively. The two FBGs should be selected in a way that the relations of $\lambda_1 + \lambda_2 \approx 2\lambda_0$ and $\lambda_1 < \lambda_0 < \lambda_2$ can be satisfied and the transmission loss of the LPFG changes linearly with the temperature at the wavelengths of λ_1 and λ_2 . The reflected light from the two FBGs possesses only single wavelength elements that are directed to a CO₂ laser-grooved LPFG from two ends of the LPFG and are received by two photodetectors, PD₁ and PD₂, respectively. Because the temperature-induced loss change of the LPFG determines the intensity of single wavelength light after passing through the LPFG, the variation of temperature can be calculated from the light intensities detected by PD₁ and PD₂.

As indicated in Fig 5, the LPFG-induced loss at some wavelengths changes linearly with the temperature. The light intensities I_1 and I_2 , detected by PD₁ and PD₂, respectively, at temperature T can be written as

$$I_1 = k_1(T - T_0) + I_{10} + \Delta(\lambda_1), \quad (2)$$

$$I_2 = k_2(T - T_0) + I_{20} + \Delta(\lambda_2), \quad (3)$$

where k_1 and k_2 are the temperature sensitivities of the LPFG-induced loss at wavelengths λ_1 and λ_2 , respectively; I_{10} and I_{20} are the light intensities de-

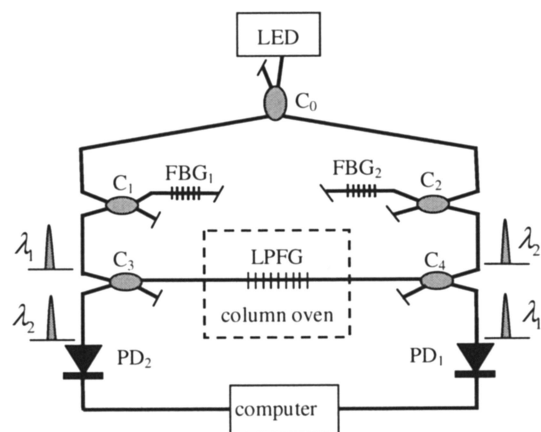


Fig. 6. Schematic of the CO₂ laser-grooved LPFG temperature sensor system based on the intensity modulation. PD₁ and PD₂ are photodetectors. C₀, C₁, C₂, C₃, and C₄ are 3 dB couplers.

ected by PD₁ and PD₂, respectively, at the room temperature of $T_0 = 20\text{ }^\circ\text{C}$; and $\Delta(\lambda_1)$ and $\Delta(\lambda_2)$ are the intensity fluctuations from the light source at wavelengths λ_1 and λ_2 , respectively. Since the two FBGs share one broadband light source with a symmetrical spectrum and $\lambda_1 + \lambda_2 \approx 2\lambda_0$, $\Delta(\lambda_1)$ is approximately equal to $\Delta(\lambda_2)$. From Eqs. (2) and (3), it follows that

$$I_2 - I_1 = (T - T_0)(k_2 - k_1) + (I_{20} - I_{10}). \quad (4)$$

Thus

$$T = T_0 + \frac{I_2 - I_1 - I_{20} + I_{10}}{k_2 - k_1}. \quad (5)$$

It can be seen from Eqs. (4) and (5) that the temperature sensitivity of the system, $(k_2 - k_1)$, is approximately twice as high as the inherent temperature sensitivity of the LPFG because k_1 is positive and k_2 is negative, as shown in Fig. 5. Thus the temperature resolution of the LPFG is effectively enhanced, which represents the prime advantage of our sensor system.

In the experiment carried out, PD₁ and PD₂ were replaced by two optical powermeters (ML910B) to directly measure the light powers corresponding to the light intensities, and a LED with a center wavelength of 1520 nm and two FBGs with Bragg wavelengths of $\lambda_1 = 1504\text{ nm}$ and $\lambda_2 = 1535\text{ nm}$ were employed. Light intensities at the room temperature of $T_0 = 20\text{ }^\circ\text{C}$ were $I_{10} = -16.52\text{ dBm}$ and $I_{20} = -10.81\text{ dBm}$. The temperature sensitivities at wavelengths λ_1 and λ_2 were $k_1 = 0.0499\text{ dBm}/^\circ\text{C}$ and $k_2 = -0.0434\text{ dBm}/^\circ\text{C}$, respectively. The LPFG employed was heated in the column oven from $20\text{ }^\circ\text{C}$ to $100\text{ }^\circ\text{C}$ in steps of $5\text{ }^\circ\text{C}$. The measured light power corresponding to the light intensities of I_1 and I_2 at the different temperatures are listed in Table 1. The values of the measured temperature in Table 1 were calculated by use of Eq. (5). It can be seen from Table 1 that the temperature accuracy of the system is close to $0.1\text{ }^\circ\text{C}$. In our experiment when the sensor head, i.e., the LPFG, is heated at a small step of $0.1\text{ }^\circ\text{C}$ in the column oven, the intensity change of I_1 and I_2 can be distinguished from the noise. So the resolution of this system is up to $0.1\text{ }^\circ\text{C}$ in the column oven.

5. Discussion

Although the resonant wavelength of a FBG is usually sensitive to the temperature, the two FBGs in our system are used to supply two light sources with a single wavelength element and are not the sensor heads embedded in the engineering structures. So the FBGs are not influenced by the temperature variation in the engineering structure measured. Of course, the FBG may be influenced by the temperature fluctuation in the surroundings. FBGs have been widely applied in sensors and communications, and some mature temperature compensation techniques have been proposed and demonstrated.^{12,13} The two FBGs in our system employed a passive temperature-

Table 1. Measurement Results Using the Proposed LPFG Temperature Sensor System

True Temperature ($^\circ\text{C}$)	Power Corresponding to I_1 (dBm)	Power Corresponding to I_2 (dBm)	Temperature Measured ($^\circ\text{C}$)
20	-16.52	-10.81	20.00
25	-16.27	-11.03	25.04
30	-15.98	-11.21	30.08
35	-15.71	-11.4	35.01
40	-15.45	-11.61	40.04
45	-15.2	-11.82	44.97
50	-14.93	-12.02	50.01
55	-14.67	-12.23	55.05
60	-14.42	-12.45	60.09
65	-14.19	-12.67	64.91
70	-13.92	-12.88	70.05
75	-13.68	-13.1	74.98
80	-13.46	-13.34	79.91
85	-13.22	-13.57	84.95
90	-13.01	-13.83	89.99
95	-12.78	-14.07	95.03
100	-12.51	-14.27	100.06

compensating package to nullify the temperature to the wavelength coefficient, as shown in Ref. 13. In this case, the grating was mounted under tension in a package comprising two materials with different thermal-expansion coefficients. As the temperature rises, the strain is progressively released, compensating for the temperature dependence of the Bragg wavelength.

The sensor head is the LPFG employed in our system and is the FBG in Ref. 5. The high temperature resolution of $0.02\text{ }^\circ\text{C}$ in Ref. 5 is attributed to the complex sensor head consisting of a FBG and an aluminum substrate, where the FGB has to be embedded in an aluminum substrate with a larger coefficient of thermal expansion to enhance its temperature sensitivity. In contrast, the sensor head in our system is only one simple LPFG. So the advantages of simple configuration and low cost exist in our system. The high temperature resolution in Ref. 14 is because the LPFG employed was fabricated in the special fiber with a high temperature coefficient of $-284\text{ nm}/^\circ\text{C}$. On the other hand, the LPFG in our system is fabricated with common optical fiber (Corning SFM-28). The double temperature sensitivity in our system is obtained from Eq. (5) by means of a differential measurement, as shown in Fig. 6.

6. Conclusions

The LPFG fabricated by use of a focused CO₂ laser beam to carve periodic grooves on the fiber exhibits unique temperature characteristics and can be used in temperature sensing. Such a system exhibits a number of advantages, such as convenient intensity measurement, double temperature sensitivity, high resolution, simple configuration, and low cost. The temperature sensing range obtained in our system is between $20\text{ }^\circ\text{C}$ and $100\text{ }^\circ\text{C}$, because of the limit of the

column oven employed, and the measurement resolution achieved is 0.1 °C. Because the CO₂ laser-fabricated LPFG is stable at high temperatures,¹⁵ our temperature sensor system has a potentially large measurement range.

This work was supported by grant G-YX51 from the Hong Kong Polytechnic University in a Postdoctoral Research Fellowship scheme and grant 60507013 from the National Science Foundation of China.

References

1. A. M. Vengsarkar, P. J. Lemaire, J. B. Judkins, V. Bhatia, T. Erdogan, and J. E. Sipe, "Long-period fiber gratings as band-rejection filters," *J. Lightwave Technol.* **14**, 58–65 (1996).
2. V. Bhatia and A. M. Vengsarkar, "Optical fiber long-period grating sensors," *Opt. Lett.* **21**, 692–694 (1996).
3. S. Khaliq, S. W. James, and R. P. Tatam, "Enhanced sensitivity fibre optic long period grating temperature sensor," *Meas. Sci. Technol.* **13**, 792–795 (2002).
4. B. H. Lee and J. Nishii, "Self-interference of long-period fibre grating and its application as temperature sensor," *Electron. Lett.* **34**, 2059–2060 (1998).
5. Y. G. Zhan, H. W. Cai, R. H. Qu, S. Q. Xiang, Z. J. Fang, and X. Z. Wang, "Fiber Bragg grating temperature sensor for multiplexed measurement with high resolution," *Opt. Eng.* **43**, 2358–2361 (2004).
6. R. W. Fallon, L. Zhang, L. A. Everall, J. A. R. Williams, and I. Bennion, "All-fibre optical sensing system: Bragg grating sensor interrogated by a long-period grating," *Meas. Sci. Technol.* **9**, 1969–1973 (1998).
7. D. D. Davis, T. K. Gaylord, E. N. Glytsis, S. G. Kosinski, S. C. Mettler, and A. M. Vengsarkar, "Long-period fibre grating fabrication with focused CO₂ laser pulses," *Electron. Lett.* **34**, 302–303 (1998).
8. Y. J. Rao, Y. P. Wang, Z. L. Ran, and T. Zhu, "Novel fiber-optic sensors based on long-period fiber gratings written by high-frequency CO₂ laser pulses," *J. Lightwave Technol.* **21**, 1320–1327 (2003).
9. Y. P. Wang and Y. J. Rao, "A novel long period fiber grating sensor measuring curvature and determining bend-direction simultaneously," *IEEE Sens. J.* **5**, 839–843 (2005).
10. C. Y. Lin, L. A. Wang, and G. W. Chern, "Corrugated long-period fiber gratings as strain, torsion, and bending sensors," *J. Lightwave Technol.* **19**, 1159–1168 (2001).
11. Y. P. Wang, Y. J. Rao, Z. L. Ran, T. Zhu, and A. Z. Hu, "A novel tunable gain equalizer based on a long-period fiber grating written by high-frequency CO₂ laser pulses," *IEEE Photon. Technol. Lett.* **15**, 251–253 (2003).
12. T. Iwashima, A. Inoue, M. Shigematsu, M. Nishimura, and Y. Hattori, "Temperature compensation technique for fibre Bragg gratings using liquid crystalline polymer tubes," *Electron. Lett.* **33**, 417–419 (1997).
13. G. W. Yoffe, P. A. Krug, F. Ouellette, and D. A. Thorncraft, "Passive temperature-compensating package for optical-fiber gratings," *Appl. Opt.* **34**, 6859–6861 (1995).
14. C. S. Shin, C. C. Chiang, and S. K. Liaw, "Comparison of single and double cladding long period fiber grating sensor using an intensity modulation interrogation system," *Opt. Commun.* **258**, 23–29 (2006).
15. G. Rego, O. Okhotnikov, E. Dianov, and V. Sulimov, "High-temperature stability of long-period fiber gratings produced using an electric arc," *J. Lightwave Technol.* **19**, 1574–1579 (2001).